Journal of Material Cycles and Waste Management (2021) 23:1855–1872
https://doi.org/10.1007/s10163-021-01256-x

ORIGINAL ARTICLE

An improved optimization model for predicting Pb recovery efficiency from residual of liberator cells: a hybrid of support vector regression and modified tunicate swarm algorithm

Fatemeh Abdolinejhad[1] · Gholam Reza Khayati[1] · Ramin Raiszadeh[1] · Nahid Sadat Yaghoobi[2] · Seyed Mohammad Javad Khorasani[3]

Received: 18 August 2020 / Accepted: 28 May 2021 / Published online: 4 June 2021

Abstract
In this study, a hybrid of support vector regression and a modified tunicate swarm algorithm (SVR-MTSA) strategy is developed to optimize the process parameters for recovery of Pb from the residual of the liberator cells. The lead recovery efficiency in the selected process was strongly nonlinear and depended on several process parameters including temperature, processing time, the content of coke, Na_2CO_3, and Fe in the precursor. The results confirmed a good agreement between the efficiencies obtained experimentally and those predicted by the model. It is also shown that using the optimal process parameters suggested by the model, achieving a Pb recovery of more than 99% was possible. Sensitivity analysis using the proposed SVR-MTSA model revealed that temperature, coke content, processing time, Na_2CO_3 amount, and Fe content of the raw material had the most significant effect on the efficiency of the lead recovery, respectively.

Keywords Lead recovery efficiency · Modified tunicate swarm algorithm · Support vector regression · Lead residual of liberator cell · Optimization

Introduction

Lead is one of the main strategic metals with significant applications in industries [1–3]. The annual lead production has experienced a growing trend recently, while the share of primary resources remained almost constant. In other words, the annual increase in lead production in recent years is due to the greater use of secondary sources. Therefore, finding new secondary sources for lead production and optimizing the recycling processes to attain higher efficiencies would play a key role in sustainable lead production in the future [4, 5].

Non-consumable anodes used in electrowinning and the liberator cells of electrorefining plants are usually made from lead-based alloys. Cold-rolled Pb anode containing 0.07–0.08 wt.% Ca and 1.35 wt.% Sn is the primary choice in the modern copper electrorefining plants [6]. The oxygen generated during the anodic reaction causes these lead anodes to corrode [7, 8]. Despite the significant progress in increasing the quality of these anodes, the corrosion of Pb–Ca–Sn anodes is one of the main problems of nearly all copper plants that use hydrometallurgical processes for copper production. This corrosion causes a large volume of sludge to form at the bottom of the liberator cells and copper electrowinning plant. This sludge contains the corrosion products of the Pb–Ca–Sn anodes. Since about twenty percent of the copper in the world is produced by hydrometallurgical methods [6], it can be imagined that a significant volume of lead-rich sludge is produced annually. Increasing environmental considerations and the feasibility of using this sludge as a secondary source for lead production encouraged factories to recycle this residual.

✉ Gholam Reza Khayati
Khayatireza@gmail.com

[1] Department of Materials Science and Engineering, Shahid Bahonar University of Kerman, P.O. Box No, 76135-133 Kerman, Iran

[2] Research & Development Center, Shahrbabak Copper Complex, National Iranian Copper Industries Company, Kerman, Iran

[3] Senior Metallurgical Engineer, Process Control Unit, Khatoonabad Copper Refinery, Shahrebabak Copper Complex, National Iranian Copper Industries Company, Kerman, Iran

In Iran, several plants use hydrometallurgical processes to produce cathodic copper. These plants produce tens of tons of lead-rich sludge per year. Accumulation of such lead-containing wastes in the open environment causes environmental severe hazards. Therefore, an effort must be made to recover this spent lead sludge. There are various approaches based on pyrometallurgy or hydrometallurgy principles for the recovery of lead wastes. Unique characteristics, such as simplicity of the process, lack of production of harmful products, and notably better recovery efficiency, caused the pyrometallurgical approaches to be preferred over the hydrometallurgical ones [3]. However, relatively high-energy consumption is one of the disadvantages of the pyrometallurgical routes, which should be addressed by maximizing the lead recovery efficiency [3].

Recently, the support vector regression (SVR), which is a powerful technique in soft computing, was employed as a regression strategy in various categories such as pattern recognition [9], novelty detection [10], and image recognition [11, 12]. Although the SVR has become more widely employed to forecast time-series data and to reconstruct dynamically chaotic systems, a useful model can only be built if the parameters of the SVR are carefully determined. Compared to other nonlinear regression techniques such as neural network [13], the SVR illustrated superior generalization performance. However, the performance of the SVR strongly depends on the selection of kernel (i.e., responsible for creating a linear or near-linear regression procedure surface, estimating the input space to the feature space, or creating a linear or near-linear regression procedure surface in the feature space and penalty (i.e., a criterion for correcting a sample that has been split incorrectly) parameters.

The main objectives of this paper are:

1. recovery of Pb from the sludge of the liberator cells in a copper refinery which uses a hydrometallurgical process;
2. proposing a modified tunicate swarm algorithm (MTSA) strategy by the addition of adaptively updating algorithm parameters to keep the balance between exploitation and exploration searches and to preserve the swarm diversity;
3. strengthening of the MTSA strategy as well as avoiding its premature convergence;
4. using an advanced SVR-MTSA model for optimizing the SVR parameters to construct an efficient SVR model with the optimal generalization performance and regression accuracy;
5. optimization of the process parameters of the recycling method, including temperature, time, coke, Na_2CO_3, and Fe contents, based on the proposed SVR-MTSA model as a real case study to maximize the efficiency of lead recovery;
6. comparison of the effect of the selected parameters on the efficiency of lead recovery using sensitivity analysis.

Background

Selection of the process for lead waste recovery

Recovery of lead waste is carried out either by pyrometallurgical or hydrometallurgical processes [1, 3, 14–17]. Compared to the pyrometallurgical processes, the hydrometallurgical ones have some disadvantages, especially in the leaching step. The consumption of a significant amount of water, the complexity of the process, formation of hazardous waste solutions, and the need to decompose lead carbonate at high temperatures to achieve the metallic lead are among these disadvantages. Thus, pyrometallurgical approaches, especially those that allow desulfurization and reduction of various lead-containing phases at high temperatures, are preferred. Considering the available resources regarding the recycling of lead-containing wastes using pyrometallurgical processes, the effect of operational parameters can be summarized as follows:

Effect of temperature and processing time on the lead recovery

According to the literature [18], during the recycling of battery residue and lead sulfates, increasing the temperature up to 1000 °C enhanced the efficiency of lead recovery. Also, the higher temperature promoted the detachment of slag from the metal and also enhanced the matte formation. The processing time was the other parameter that affected the lead recovery. Reducing the processing time less than the optimal value decreased the lead recovery efficiency due to the lack of sufficient time for the reaction between the precursors. Prolonging the processing time increased the likelihood of lead oxidation and its entry to the slag phase, which significantly decreased the efficiency of lead recovery.

Effect of Na_2CO_3 content

If the waste contains sulfide phases of lead, the amount of sodium carbonate in the precursor affects the efficiency of lead recovery due to its role in the reduction of $PbSO_4$ to Pb in reaction (1) [15]:

$$PbSO_{4(s)} + Na_2CO_{3(s)} + C_{(s)} = Pb_{(l)} + Na_2SO_{4(l)} + CO_{(g)} + CO_{2(g)} \quad (1)$$

Effect of coke content

High carbon content in the precursor decreases the efficiency of lead recovery due to the increase of sulfur and lead content of the slag. From the thermodynamic point of view, carbon initially reduces the lead oxide according to the following stoichiometric reaction [15]:

$$5PbO + 2.5C = 5Pb + 2.5CO_2 \quad (2)$$

If the carbon content is higher than the above stoichiometric requirement, reaction (3) will start:

$$PbSO_4 + 2C = PbS + 2CO_2 \quad (3)$$

In this case, the potential for the formation of lead sulfide, i.e., a decrease in the efficiency of lead recovery, is enhanced [18].

Effect of iron addition

As shown in reaction (3), the formation of PbS at about 650 °C is inevitable if the amount of carbon in the precursor is too high. In this case, Fe can reduce the lead sulfide to Pb according to reaction (4). This reaction is activated at about 900–1000 °C [2].

$$PbS + Fe = Pb + FeS \quad (4)$$

As shown above, lead could be present in the process as various phases, including PbS, $PbSO_4$, and PbO. There are many parameters, i.e., presence and amount of coke, iron and sodium carbonate as reducing agents, and also processing time and temperature, each of which can affect the final product of the process to some extent. Therefore, it is necessary to use an appropriate optimization algorithm to optimize the process parameters to achieve the highest recovery efficiency.

Support vector regression (SVR)

The support vector machine (SVM) algorithm is a popular machine learning approach that can also be used as a regression method. In other words, the support vector regression (SVR) considers the same features of SVM for classification and has only minor differences. For example, the output of the regression problem is a real number, and so estimating a value that has infinite possibilities is difficult. Nevertheless, the main principles are the same, and it tries to minimize error and individualize the hyperplane, which maximizes the margin. Due to the excellent generalization performance of SVR, it has been widely used in different fields such as face recognition, feature selection, and prediction [9–13].

SVR technique determines the suitable structure with some complexity to the available small size samples during the optimization. It shows a strong generalization ability and dimension independence, which makes it superior to traditional machine learning algorithms. In nonlinear regression, the SVR kernel function is necessary to project the input space into the feature space or create a linear or nearly linear regression hypersurface in the space of the features. The setting of the SVR parameter (i.e., penalty parameter C, the kernel function parameter δ, smoothness response parameter ε) has a great influence on the performance of the SVR [13].

In this paper, a novel approach based on the tunicate swarm algorithm (TSA) for parameter optimization of the SVR is proposed to improve the prediction accuracy of the model.

Tunicate swarm algorithm

Meta-heuristic optimization strategies have outstanding specifications including (i) employing easy concepts with easy implementation; (ii) no need for gradient information; (iii) ability to find a globally optimal, and (iv) adaptable for various problems such as engineering applications. Hence, these strategies are considered as good candidates for optimization of problems. In this paper, a new meta-heuristic optimization algorithm, namely, a tunicate swarm algorithm (TSA) is used since it can find better optimal solutions than other competitive strategies and is suitable for solving the real case engineering design problems [19, 20].

At sea, tunicates use two strategies to find the optimal state in their surroundings to find food, i.e., swarm intelligence and jet propulsion. A tunicate must meet three primary conditions when moving with a jet propulsion behavior: (i) should not conflict with the other tunicates in the search space, (ii) should choose the right path to the best search position, and (iii) should get as close as possible to the best search agent. Simultaneously, swarm behavior updates the position of other tunicates for the best optimal solution. In summary, the mathematical model for satisfying these conditions is explained as follows.

Avoiding conflicts among search agents

To prevent confrontation of tunicates with each other, a new search agent position is defined using $\vec{A}$, $\vec{G}$, and $\vec{M}$ vectors as Eqs. (5), (6) and (7(:

$$\vec{A} = \frac{\vec{G}}{\vec{M}} \quad (5)$$

$$\vec{G} = c_2 + c_3 - \vec{F} \quad (6)$$

$$\vec{F} = 2 \cdot c_1 \tag{7}$$

in which, $\vec{G}$ indicates the gravity forces, $\vec{M}$ is social forces, and $\vec{F}$ is water flow advection in the deep ocean. c_1, c_2, and c_3 are random values in the range of [0, 1]. $\vec{M}$ can be estimated using Eq. (8).

$$\vec{M} = [P_{\min} + c_1 \cdot (P_{\max} - P_{\min})] \tag{8}$$

in which, $P_{\min}$ and $P_{\max}$ are the initial and subordinate speeds to construct the social interaction. Note that the values of $P_{\min}$ and $P_{\max}$ are considered as 1 and 4, respectively, by the authors in [20].

Moving to the best neighbor direction

The tunicates should move towards the best neighbor direction based on Eq. (9):

$$\vec{PD} = \left|\vec{FS} - r_{and} \cdot \vec{P}_p(x)\right| \tag{9}$$

in which, the distance between the tunicate and the food source is defined by $\vec{PD}$, x is the current iteration, the optimal food source position is determined by $\vec{FS}$, the position of the tunicate is depicted by $\vec{P}_p(x)$, and r_{and} is a random number in the range of [0, 1].

Converging towards the best search agent

The updated position of the tunicate in respect to the position of the food source, as the best search agent can be determined by Eq. (10):

$$\vec{P}_p(x) = \begin{bmatrix} \vec{FS} + \vec{A} \cdot \vec{PD}; & if : r_{and} \geq 0.5 \\ \vec{FS} - \vec{A} \cdot \vec{PD}; & if : r_{and} < 0.5 \end{bmatrix}. \tag{10}$$

Swarm behavior

To simulate the behavior of tunicates, initially, the best solutions between the first two optimal are determined. Then, by considering the position of the best tunicate, the positions of other search agents are updated. The swarm behavior of the tunicates can be estimated by Eq. (11).

$$\vec{P}_p(\vec{x} + 1) = \frac{\vec{P}_p(x) + P_p(\vec{x} + 1)}{2 + c_1}. \tag{11}$$

The proposed method

First, a modified tunicate swarm algorithm (MTSA) is introduced to enhance the global and local search ability of the standard TSA. Second, an SVR-MTSA model is developed to optimize the SVR parameters by MTSA approach, since the quality of the model built by the SVR [19] mostly depends on the careful tuning of its parameters. Finally, the optimal values of features from the lead recovery dataset are determined in such a way that the efficiency of lead recovery is maximized based on the SVR-MTSA.

Modified tunicate swarm algorithm (MTSA)

In the original TSA, $\vec{A}$, $\vec{G}$, and $\vec{F}$ are the vectors that enable the search agents to scan the search space randomly without having any conflicts. Variation in these vectors provides the possibility of better exploration and exploitation phases. In respect to other evolutionary optimizers, the original form of TSA, especially when it has a higher dimension and complexity, can get trapped in local optimum solutions. Under this condition, finding the global optimal would face a severe challenge. In this research, the original TSA is improved in two aspects:

(i) Self-adaptive parameters: Since the settings of the meta-heuristic algorithm must be adjusted based on each type of problem, the process becomes time-consuming and constitutes a significant burden on the user's part. Therefore, the proposed algorithm adopts the controlling parameters to the circumstances of the tunicates at a specific moment.
(ii) Improving exploration ability: The proposed algorithm changes the direction of the movement for tunicates so that they not only move towards the best search agent but also search for other directions to enhance their exploration phase.

Self-adaptive parameters

In the standard TSA, the value of parameter A (which affects the agents' searching process) depends on several random variables (i.e., c_1, c_2, and c_3) and so with selecting inappropriate values for these parameters, the method cannot reach to a global optimum. Therefore, we pursue a way to remove these variables and modify parameter A to depend on a more reliable value. The details of the modification of parameter A is explained in detail as follows:

$\vec{A}$ can be written as

$$\vec{A} = \frac{c_2 + c_3 - \vec{F}}{P_{\min} + c_1(P_{\max} - P_{\min})}, \tag{12}$$

$$\vec{A} = \frac{c_2 + c_3 - (2c_1)}{P_{\min} + c_1(P_{\max} - P_{\min})} = \frac{c_2 + c_3 - c_1}{P_{\min} + c_1(P_{\max} - P_{\min})}. \tag{13}$$

In the original form of TSA [20], the values of $P_{\min}$ and $P_{\max}$ are set to 1 and 4, respectively. c_1, c_2, and c_3 are constants that are randomly distributed through [0, 1]. Therefore, assuming the interval of these random parameters $\vec{F}$ in Eq. (5) and $\vec{M}$ in Eq. (7) can be considered to change in [−2, 2] and [1, 4] intervals, respectively. Also, $\vec{A}$ vector affects both exploitation and exploration phases [20]. Hence, the variation of $\vec{A}$ provides the possibility of the step jump of solutions through the search space (as shown in Eq. (5)). In the current study, values of the numerator and the denominator are adjusted high and low for the first iterations. This adjustment enabled the search agents to make long step jumps and explore a wider area of search space. Also, increasing the iteration number, caused $\vec{A}$ to decrease to lower values (i.e., high value for the denominator and low value for the numerator). These modifications enhance the exploitation phase and local searches. The modified version of $\vec{A}$ can be expressed as Eq. (14).

$$\vec{A} = \frac{2 - 4(t/t_{\max})}{4 - 3(t/t_{\max})}, \tag{14}$$

in which, t and $t_{\max}$ are the current number and the maximum number of iterations, respectively.

Improve exploration ability

As shown in Eq. (10), all tunicates (i.e., search agents) are moved towards the food source (i.e., best search agent). In other words, the tunicates are concentrated on the local search and so balancing between exploration and exploitation is necessary. To enhance the exploration phase in the current study, Eq. (14) was used to estimate $\vec{A}$ value. If $\vec{A}$ is higher than 1.25, then finding of the food source (i.e., exploration) is restricted to the neighborhood of the solution selected by the random strategy. Otherwise (i.e., $\vec{A}$ is lower than 1.25), the neighborhood of the best solution so far is exploited. This process is continued to a preset maximum iteration. Figure 1 illustrates the flowchart of the proposed MTSA.

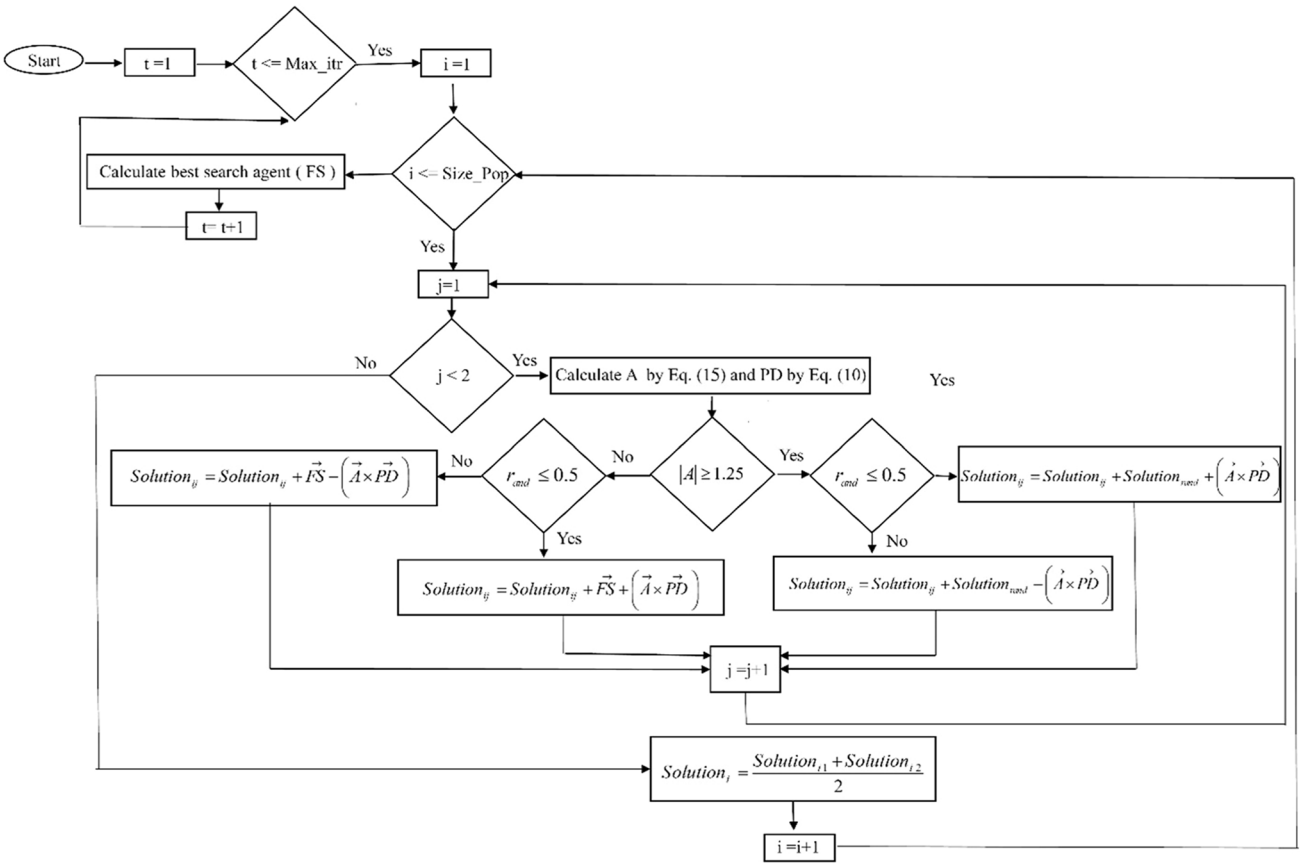

Fig. 1 Flowchart of the proposed MTSA

Parameter optimization of SVR by MTSA

The performance of the SVR strongly depends on the adequate calibration of its parameters (i.e., penalty, C, kernel, δ, and smoothness response, ε). In the original SVR, these parameters are adjusted either by trial and error or by empirical experiments. However, the computational cost is increased exponentially according to the number of parameters and the number of sampling points for each parameter. Recently, meta-heuristic techniques (e.g., genetic algorithm (GA) and particle swarm optimization (PSO)) have been used to optimize the SVR parameters for better global search abilities against numerical optimization strategies. In this work, MTSA was applied for the selection of the SVM parameters. The population of the solutions (i.e., solutions for the SVR parameters) is generated by the MTSA and SVRs are built with each solution. Then, they are trained, and their parameters are evaluated in the test stage. In this research, we mainly concentrated on the parameter optimization of the SVR to minimize the prediction error and proposed an SVR-modified tunicate swarm algorithm (SVR-MTSA).

For generating the population of solutions, the search space dimension must be calculated. The search space of the problem for optimization of the SVR parameters has three dimensions (i.e., ε, C, and δ). For the i_{th} tunicate, y_i is the corresponding predicted value by $x_i = (x_{i\varepsilon}, x_{iC}, x_{i\delta})$ in the best position of x_i. The solutions are coded with real values. For testing the created SVRs, a cross-validation technique is used, which is a popular technique for the estimation of the generalization error. The K-fold cross-validation is a kind of cross-validation that is a popular technique for the evaluation of model. The main idea of this method is that all observations participate in the testing process. In K-fold cross-validation, the dataset is divided into k parts and one part is applied for validation. Then, the remaining parts are considered for training. Figure 2 indicates the tenfold cross-validation that is used in this paper.

In each iteration, SVR-MTSA tries to fit the training folds. Eventually, the final fitness is calculated based on the average of the values obtained by the validation sets. One of the main advantages of this technique over the usual division of the data set into two parts (i.e., test and train) is that the pessimistic bias is reduced by considering more training data in contrast to setting aside a relatively large part of the dataset as the test set. Then, the generalization error is determined as the mean of the test errors in the k experiments. In the current study, the dataset is divided into three folds, i.e., testing, validation (calculating the performance fitness of the model), and training. The correlation coefficient (R^2, Eq. (15)), mean absolute percentage error (MAPE, Eq. (16)), mean bias error (MBE, Eq. (17)), and root mean square error (RMSE, Eq. (18)) are used as criteria for the evaluation of the investigated models. Generally, the closer to zero the MAPE, MBE,

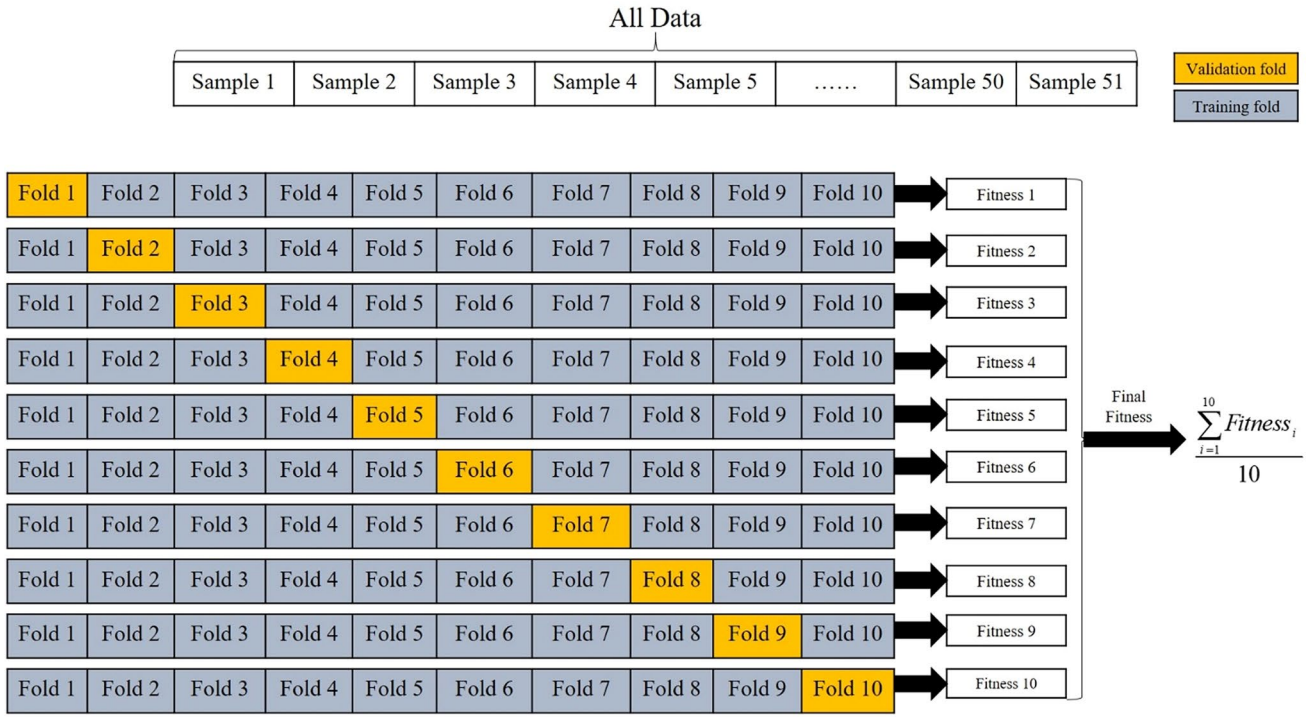

Fig. 2 10-fold cross-validation process

and RMSE values, the higher the accuracy of the models. A closer R^2 to unity is more favorable if R^2 is considered the criterion for the accuracy of the models [21].

$$R^2 = 1 - \frac{\sum_{i=1}^{n} (y_k - f(x_k, w))^2}{\sum (y_k - \bar{f}(x_k, w))^2}, \tag{15}$$

$$\text{MAPE} = \frac{1}{n}\left[\sum_{i=1}^{n} \frac{(y_k - f(x_k, w))}{f(x_k, w)}\right] \times 100, \tag{16}$$

$$\text{MBE} = \frac{1}{n}\left[\sum_{i=1}^{n} (y_k - f(x_k, w))\right], \tag{17}$$

$$\text{RMSE} = \left[\sum_{i=1}^{n} \frac{1}{n}(y_k - f(x_k, w))^2\right]^{\frac{1}{2}}. \tag{18}$$

The RMSE metric (Eq. (18)) can be used to define the performance index (i.e., *fitness*) of the models.

The *fitness* for the *i*th agent is calculated by Eq. (19), where RMSE_{max} indicates the highest RMSE value for the agents in the population with n agents.

$$\text{Fitness}_i = \frac{\text{RMSE}_{\text{max}} - \text{RMSE}(I_i)}{\sum_{j=1}^{n} (\text{RMSE}_{\text{max}} - \text{RMSE}(I_j))}. \tag{19}$$

Figure 3 illustrates the flowchart of the SVR-MTSA.

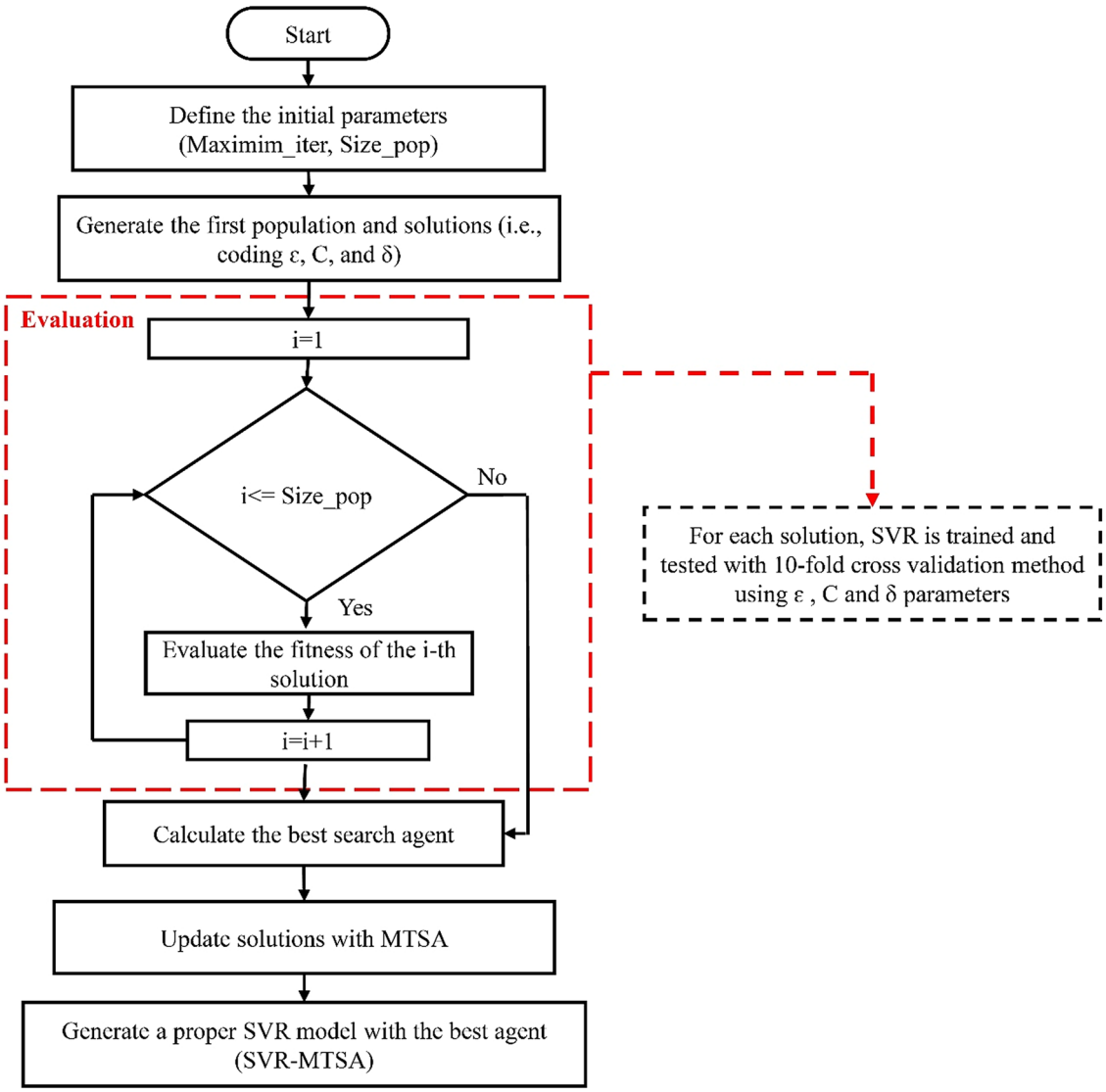

Fig. 3 Flowchart of the SVR-MTSA

At the end of the iterations, the optimized SVR, which achieved the lowest error (the best fitness), is considered as the SVR-MTSA.

Determination of the optimized values for the selected practical features

The recovery of lead from a secondary source is chosen as an engineering example for finding the optimal value for the lead recovery, based on the SVR-MTSA approach. The main steps of the optimization process with the SVR-MTSA approach is shown in Fig. 4.

The optimization process is carried out in two main steps:

(1) The best values for the SVR parameters (i.e., ε, C) and the radial basis function kernel (i.e., δ) is determined using the MTSA strategy. In this step, the empirical values are selected as input for temperature, processing time, and the amount of reducing agents (coke, Fe, and Na_2CO_3). The efficiency of Pb recovery, which should be maximized, is calculated as output;
(2) The optimum values of the process parameters to attain the highest recovery efficiency is achieved by the obtained SVR-MTSA.

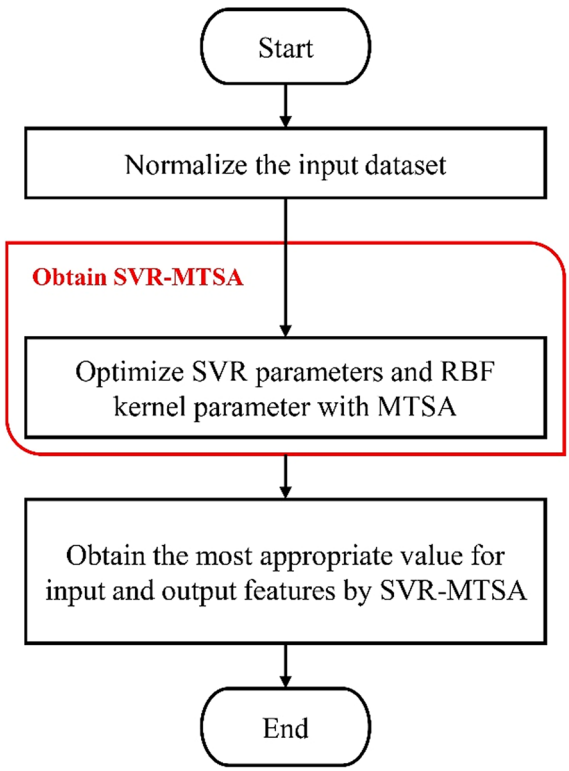

Fig. 4 General steps of the SVR-MTSA strategy

As was mentioned earlier, the MTSA is the enhanced version of the original form of the TSA strategy with two additional improvements (i.e., adoption of a self-adaptive method and an improved exploration phase). Each column of tunicates is analog to one parameter of the experimentally collected dataset, and hence the number of columns is equal to the number of recovery process parameters. A random number between the minimum and maximum values of the corresponding recovery process parameters in the selected dataset is used for the initialization of the tunicate. Then the evaluation of fitness for solutions is carried out by the proposed SVR-MTSA model. Figure 5 shows the steps carried out for the optimization of the parameters based on MTSA and SVR-MTSA.

The ability of the SVR-MTSA for the optimization of the efficiency of Pb recovery is also compared to those of back-propagation neural networks (BPNN), original SVR-cross-validation, SVR with basic TSA (SVR-TSA), SVR

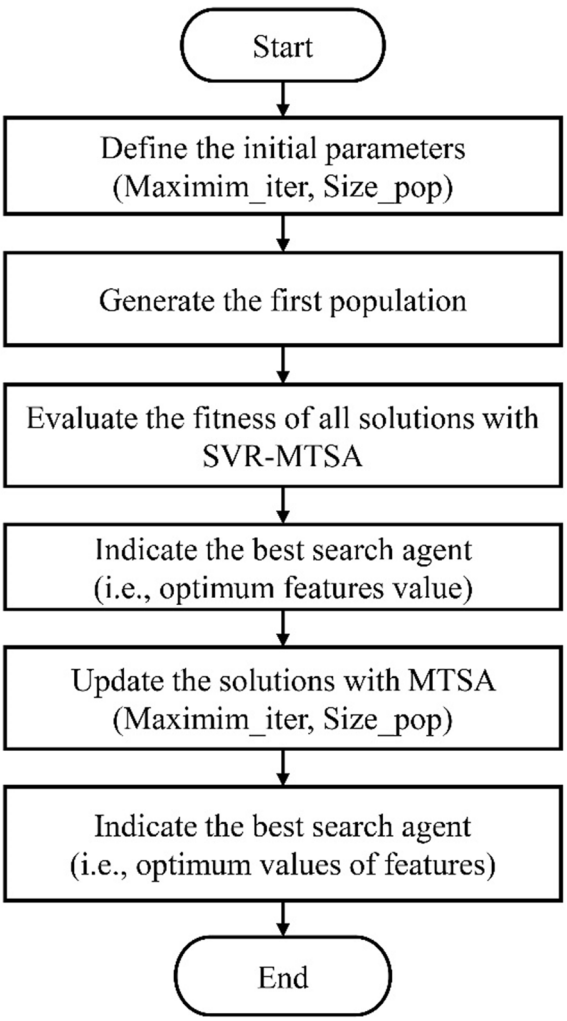

Fig. 5 Optimization of the parameters with MTSA and SVR-MTSA

with grey wolf optimization algorithm (SVR-GWO), SVR with particle swarm optimization (SVR-PSO) and SVR with multi-verse optimizer (SVR-MVO) models.

Experimental method

Lead-rich waste of the liberator cells in the electrorefining plant of Khatoonabad copper refinery in Shahrebabak, Iran, was selected as the secondary source for lead recovery. The identity of the phases in this waste was determined using XRD (Philips, X'pert-MPD system by Cu-K_α) and XRF (Phillips, 1404) techniques. Recycling was carried out based on a pyrometallurgical process. In this process, the mixture of coke (provided by Zarand Iranian Steel Company), steel turning chips, and Na_2CO_3 (produced by Kaveh Soda Chemical Industries Company) was heated to different temperatures for different periods. The levels selected for these parameters are summarized in Table 1.

A mixture of precursors was placed in a cast-iron crucible in an electric furnace pre-heated to a preset temperature. After the processing time, the crucible was removed from the furnace, and the melt was poured into a steel mold after the slag was removed. To determine the lead recovery efficiency, the solidified ingot was weighted using a digital scale with 0.0001 g accuracy, and its chemical composition was measured using a mass spectrometry technique.

In this study, D-optimal array, i.e., one of the most common design of experiments (DOE) techniques [22–27], was used to determine the schedule of experiments. This technique suggested the performance of 102 trials (Table 2), instead of 36,864 (based on the full factorial design(, without affecting the accuracy of the collected dataset [21].

Results and discussion

Table 3 shows the efficiency of lead recoveries in various experiments carried out in this research with various process parameters denoted in Table 2.

Table 3 shows that the process parameters greatly influenced the lead recovery and caused it to vary between 2 and 98%. The bivariate (Pearson) correlation analysis is used to find the correlation between the selected process parameters. It is necessary to note that if the process parameters have significant correlation coefficients due to the incorrect exaggeration of each parameter and the evolution of multicollinearity, then the proposed model would not have a high accuracy [26]. Figure 6 shows the correlation matrix of the process parameters. As shown, the correlation coefficient between any two process parameters is less than 0.125, and therefore, there is no significant correlation between any of the selected parameters.

Table 1 The selected levels for each process parameter

Variable	Level 1	Level 2	Level 3	Level 4
Temperature (°C)	850	900	950	1000
Time (min)	60	90	120	–
Fe (g in 100 g residue)	0	5	10	12
Coke (g in 100 g residue)	6	10	14	22
Na_2CO_3 (g in 100 g residue)	6	10	18	22

Phase analysis of Pb-rich waste

The concentration of phases present in the lead-rich waste of the liberator cells, measured by XRF, is shown in Table 4. The XRD spectrum obtained from this waste is also shown in Fig. 7. These results confirmed the main phases present in the waste to be As_2O_3, Sb_2O_3, PbO, and $PbSO_4$.

According to the literature [2, 23], reduction of PbO, PbS, and $PbSO_4$ were carried out by coke, Fe, and Na_2CO_3, respectively, and hence, determination of the amount of these phases for the start of the optimization process was essential. During the selection of the minimum and maximum levels of the reducing agents, all the Pb was supposed to be in the form of PbO and $PbSO_4$.

SVR-MTSA modeling

Figure 8 shows the change of fitness versus iteration for different meta-heuristic strategies. Based on the criteria for the evaluation, i.e., RMSE, MAPE, R^2, and MBE, the figure shows that the SVR-MTSA outperformed the BPNN and other variations of the SVR model.

All the curves had a descending trend, which is typical for optimization algorithms. At the start of the iteration process, this decreasing trend was more significant for the SVR-TSA and SVR-MTSA strategies. Due to the exploitation process, the fitness curve of SVR-MTSA decreased more smoothly. It can be concluded that the SVR-MTSA strategy can effectively be balanced between exploitation and exploration compared to SVR-TSA using a new updating strategy. Finally, the results indicated that the fitness of the SVR-MTSA model could achieve 6% better than SVR-TSA and 11% better than SVR-GWO. One of the reasons for this superiority is because MTSA balances between exploration and exploitation by changing the corresponding variable and the number of iteration while GWO sets this variable by a random number.

Figure 9a represents the RMSE (Eq. (18)) versus iteration number for various models. As mentioned, a model with higher accuracy has a smaller RMSE value. It can be seen that the SVR-MTSA had a fast convergence speed and could reach to the lowest RMSE due to its ability to search the

Table 2 Details of the experiments carried out in this study, Fe, coke, and Na_2CO_3 are in g per 100 g precursor

Exp	Temp (°C)	Time (min)	Fe	Coke	Na_2CO_3	Exp	Temp (°C)	Time (min)	Fe	Coke	Na_2CO_3
1	850	120	12	14	6	52	800	90	12	14	14
2	1000	120	0	22	18	53	850	90	0	22	22
3	950	60	10	22	22	54	850	90	5	22	6
4	900	120	12	14	10	55	800	60	0	10	10
5	800	120	5	10	6	56	800	60	0	18	10
6	850	90	10	10	14	57	850	60	0	18	10
7	900	90	10	22	6	58	1000	90	0	22	10
8	900	120	5	6	22	59	950	60	5	18	14
9	850	90	12	10	18	60	800	60	10	18	18
10	1000	120	12	22	18	61	800	60	5	18	22
11	1000	90	0	6	6	62	900	60	0	18	6
12	1000	120	5	18	10	63	1000	90	10	22	14
13	850	90	5	22	18	64	950	120	0	10	10
14	1000	120	12	18	18	65	1000	120	10	14	6
15	900	120	10	18	14	66	900	60	0	14	18
16	850	120	10	14	14	67	950	120	5	10	6
17	850	90	5	6	18	68	850	90	12	6	6
18	800	60	10	14	14	69	950	120	0	22	22
19	1000	90	10	14	6	70	950	120	10	14	10
20	950	90	12	6	14	71	800	90	0	18	14
21	800	90	0	10	10	72	800	120	10	18	18
22	850	60	0	6	6	73	1000	60	10	22	22
23	850	60	0	10	18	74	900	120	12	6	18
24	850	120	12	14	14	75	850	60	10	6	6
25	850	60	5	22	14	76	950	90	5	22	10
26	800	90	12	6	10	77	1000	120	5	14	14
27	1000	60	0	14	6	78	800	90	12	22	6
28	900	120	0	22	18	79	850	90	5	18	18
29	1000	60	0	6	22	80	850	90	5	18	14
30	900	120	10	10	18	81	800	90	5	14	6
31	900	120	5	6	18	82	850	60	12	18	18
32	950	60	10	22	10	83	850	90	10	18	18
33	800	60	0	18	18	84	950	120	12	10	10
34	850	120	12	18	18	85	900	60	10	22	10
35	850	120	5	22	18	86	950	60	12	10	14
36	800	120	0	6	10	87	950	60	0	6	22
37	1000	120	5	22	10	88	800	90	10	10	10
38	1000	60	12	22	10	89	850	60	12	10	14
39	1000	60	5	14	6	90	800	90	0	10	6
40	950	120	5	10	22	91	950	90	5	10	18
41	800	90	0	18	6	92	950	60	0	10	14
42	950	60	12	14	6	93	800	60	10	10	6
43	800	60	12	18	14	94	800	60	5	6	18
44	900	120	10	6	6	95	900	90	12	18	18
45	1000	60	10	18	14	96	950	90	5	6	22
46	950	60	5	10	6	97	1000	90	0	6	14
47	950	90	12	10	18	98	900	60	5	10	18
48	850	90	0	14	18	99	950	60	0	22	6
49	1000	90	0	18	6	100	850	60	12	10	10
50	850	120	12	22	14	101	900	90	12	22	22
51	800	120	5	10	22	102	1000	60	0	22	22

Table 3 Lead recovery, in % with a measurement accuracy ± 1%, obtained in the experiments denoted in Table 2

Exp	Recovery	Exp	Recovery	Exp	Recovery	Exp	Recovery	Exp	Recovery	Exp	Recovery
1	98	18	51	35	90	52	70	69	11	86	96
2	24	19	22	36	63	53	67	70	24	87	77
3	96	20	11	37	31	54	73	71	50	88	65
4	13	21	49	38	12	55	33	72	83	89	68
5	72	22	46	39	99	56	35	73	11	90	48
6	80	23	49	40	17	57	49	74	13	91	2
7	95	24	99	41	49	58	8	75	63	92	77
8	2	25	58	42	96	59	86	76	2	93	49
9	84	26	68	43	55	60	52	77	31	94	42
10	44	27	91	44	8	61	45	78	70	95	99
11	4	28	96	45	9	62	63	79	74	96	2
12	31	29	91	46	84	63	25	80	73	97	6
13	74	30	10	47	12	64	7	81	57	98	71
14	43	31	1	48	65	65	38	82	70	99	78
15	11	32	95	49	7	66	64	83	82	100	67
16	96	33	36	50	2	67	14	84	27	101	2
17	71	34	0.5	51	74	68	81	85	80	102	94

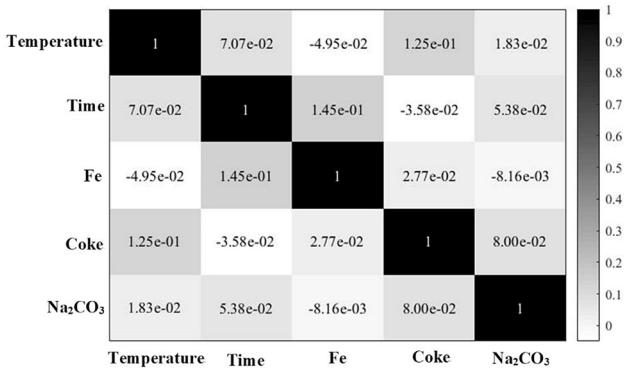

Fig. 6 The correlation matrix of selected process parameters in the current study

most promising areas. Moreover, the SVR had a superior generalization performance compared to the neural network in a regression problem [27]. As shown in Fig. 8b, the efficiency of Pb recovery is enhanced after 200 iterations due to the effective scanning of search spaces by the proposed model.

Figure 10 shows the change in the correlation coefficient, R^2, versus iteration number for different optimization algorithms. The closer to unity the R^2 value, the higher the accuracy of the optimization method. Figure 10 revealed that the SVR-MTSA had the highest R^2 value. The high accuracy of the MTSA algorithm can be attributed to the fact that it is not limited to the local optimal values and explores the entire search space. In other words, the MTSA generates the best optimal solution and continuously improves the solution by changing the direction of the movement of the tunicates, which enhances its exploration ability. Figure 11 summarizes the various statistical criteria for evaluating the accuracy of the three variations of the proposed SVR model, named MTSA-SRV1, MTSA-SRV2, and SVR-MTSA3 with three different kernels, i.e., Gaussian, linear and polynomial, respectively. Based on all the accuracy criteria, this figure determined the SVR-MTSA1 model to have the most accurate kernel.

Validation test

A test with the optimal process parameters suggested by the SVR-MTSA model (shown in Table 5) to achieve the highest Pb recovery is carried out to evaluate the accuracy of the proposed model. The model suggested this experiment to gain a 99.96% recovery. The result of the test showed

Table 4 Concentration of phases present in the lead-rich waste of the liberator cells, determined by XRF

Compound	wt.%	Compound	wt.%	Compound	wt.%	Compound	wt.%
PbO	55.3	Bi_2O_3	2.5	K_2O	0.1	NiO	0.1
SO_3	15.6	Fe_2O_3	2.4	CaO	0.1	Cl	< 0.01
As_2O_3	9.9	SnO_2	0.6	MgO	0.2	P_2O_5	< 0.01
Sb_2O_3	12.5	Al_2O_3	0.35	SiO_2	0.35	Na_2O	< 0.01

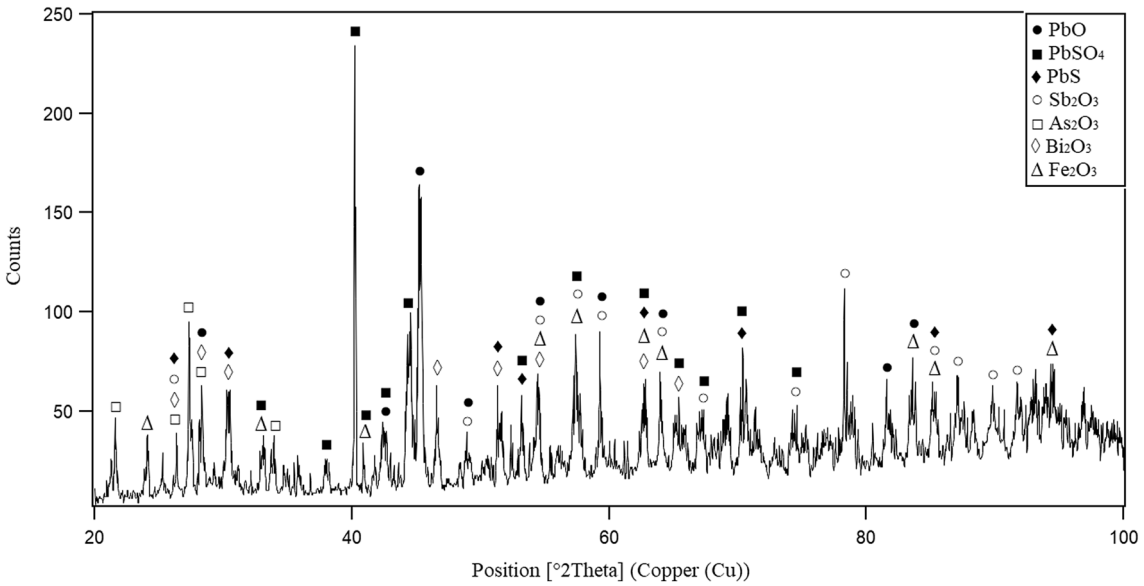

Fig. 7 XRD spectrum obtained from the lead-rich waste of the liberator cells

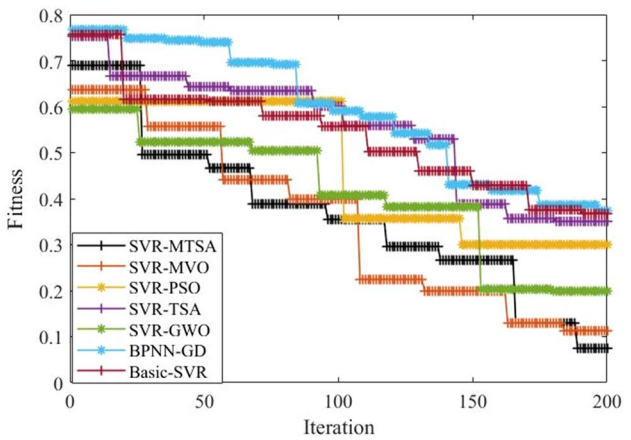

Fig. 8 Changes of fitness versus iteration for different meta-heuristic strategies

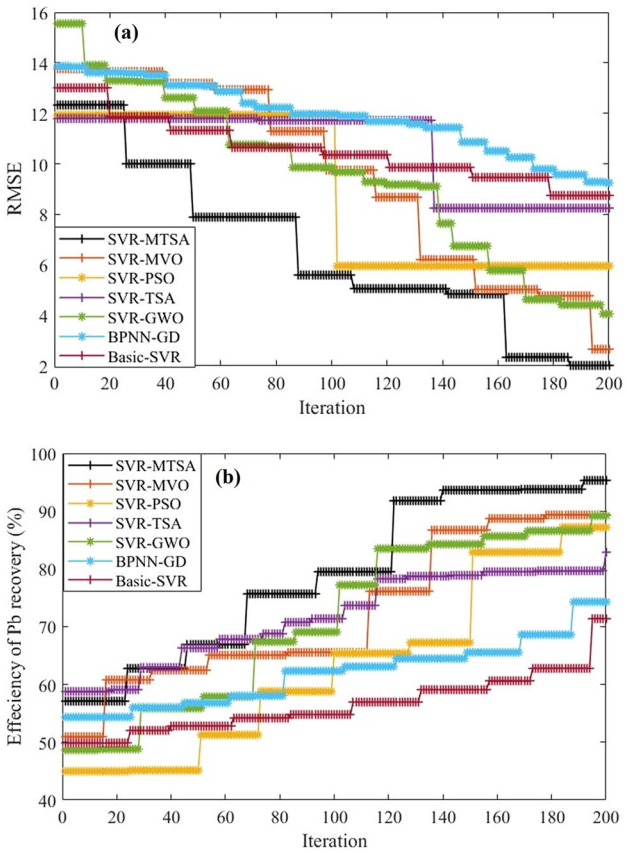

Fig. 9 Comparison of **a** RMSE and **b** the efficiency of the meta-heuristic strategies on predicting the efficiency of lead recovery as a function of iteration number

the recovery to be about 99%, a good agreement with the predicted value.

As shown in Table 6, For 100 iterations, SVR-GWO has better performance in terms of fitness whereas SVR-MTSA is the second best optimizer. With the increasing number of iterations (i.e., 200), the modified parameter *A* helps to the proposed SVR-MTSA and can escape from local optima and reach to a better fitness compared to when the number of iteration is set to 100.

The output does not always indicate better convergence and diversity because sometimes the result obtained may be different from the optimal solution. The Wilcoxon signed-rank test [28] is performed for the average value of the fitness values and R-squared. In each metric, the difference

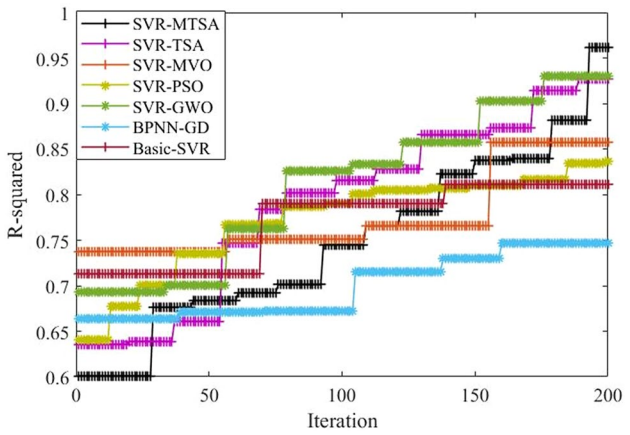

Fig. 10 Correlation coefficient, R^2, versus iteration number for different optimization algorithms

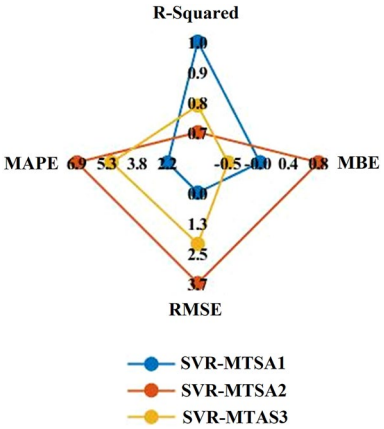

Fig. 11 Statistical criteria for evaluating the accuracy of MTSA-SRV1, MTSA-SRV2 and SVR-MTSA3 models with Gaussian, linear and polynomial kernels, respectively

between the mean results is calculated for each pair. Then, these differences are arranged in an ascending order and if the proposed technique is better than the competitor method, the positive rank is obtained. Table 6 presents the Wilcoxon test, where +, −, and = represent that the output of SVR-MTSA is superior, inferior, and equal to competitor techniques, respectively. From Table 7, it is observed that SVR-MTSA outperforms all the competitor algorithms except SVR-GWO, which finds superior for fitness and R-squared when iteration is set to 100. For 200 iterations, the proposed method (i.e., SVR-MTSA) reaches better fitness value in average compared to other techniques.

We used two more criteria namely variance accounted for (VAF in Eq. (20)) and Median of Absolute errors (MedAE in Eq. (21)) to better show the performance of competitive algorithms.

$$\mathrm{VAF} = \left[1 - \frac{\mathrm{var}(y - \hat{y})}{\mathrm{var}(y)}\right] \times 100, \tag{20}$$

$$\mathrm{MedAE} = \mathrm{median}(y - \hat{y}), \tag{21}$$

where y is the actual output and $\hat{y}$ is the output predicted by the suggested model. In addition, $\bar{y}$ indicates the average of the actual outputs.

From Fig. 12, it can be seen that the proposed algorithm (i.e., SVR-MTSA) improves VAF by 7.2% and 6.5% compared to SVR-GWO and SVR-TSA, respectively. A model with a high value for VAF parameter means that it has been able to predict the output with high accuracy. The SVR where the parameters are optimized with GWO has better performance until the 170th iteration compared to SVR-MTSA and then it falls into the local optimum due to the lack of local search operator. While the proposed MTSA helps SVR to achieve an appropriate value for Gaussian kernel and reduce error.

Figure 13 illustrates the median of absolute errors for various methods over 200 iterations. This parameter indicates the oscillation of errors. According to this parameter, a model with higher accurate prediction obtains lower error oscillation. The SVR-MTSA improves MedAE compared to Basic-SVR and BPNN-GD by 27.6% and 32.8%, respectively. Back propagation neural network and basic support vector regression use gradient descent to optimize neural network weights and SVR parameters. The gradient descent easily traps on local optimal [29] and suffers from the weak exploration operations. While by training the SVR with MTSA, the better result is achieved since it has better exploration activities in SVR-MTSA than these two algorithms.

The efficiency of the Pb recovery obtained experimentally was compared to those predicted by the SVR-MTSA model for the variation in processing time, temperature, coke, Fe, and Na_2CO_3 contents. The results, shown in Fig. 14a–e, respectively, showed a good agreement between these two

Table 5 The optimal process parameters suggested by the SVR-MTSA model to obtain the highest Pb recovery, and the recovery obtained by the model and experimentally

Temp (°C)	Time (min)	Coke (g/100 g)	Fe (g/100 g)	Na_2CO_3 (g/100 g)	Recovery (%)	
					Experiment	Prediction
990	110	11	21	14.5	99	99.96

Table 6 Comparison of the performance of the SVR-MTSA algorithm with six other optimization algorithms

Methods	Metrics	Fitness		R^2	
		100 iterations	200 iterations	100 iterations	200 iterations
SVR-MTSA	Ave	0.3376	**(0.0738)**	0.7711	**(0.9638)**
	Std	0.0052	0.0031	0.1793	0.0054
SVR-TSA	Ave	0.5189	0.3791	0.7871	0.9108
	Std	0.0268	0.0194	0.0875	0.1865
SVR-GWO	Ave	**(0.3317)**	0.2634	**(0.8369)**	0.9173
	Std	0.0004	0.0275	0.2357	0.1809
SVR-PSO	Ave	0.3861	0.3078	0.7466	0.8152
	Std	0.0012	0.0855	0.0076	0.0811
SVR-MVO	Ave	0.3981	0.1235	0.7600	0.8439
	Std	0.0027	0.0434	0.1790	0.0018
Basic-SVR	Ave	0.6092	0.3968	0.7503	0.7978
	Std	0.1381	0.0813	0.0698	0.0549
BPNN-GD	Ave	0.5973	0.3990	0.6748	0.7117
	Std	0.1276	0.0726	0.0038	0.0925

The best value for each criterion is denoted by parentheses (bold)

Table 7 Wilcoxon signed-rank test

Algorithms	Fitness		R^2	
	100 iteration	200 iteration	100 iteration	200 iteration
SVR-MTSA	+	+	+	+
SVR-TSA	+	+	=	+
SVR-GWO	−	+	−	+
SVR-PSO	+	+	+	+
SVR-MVO	+	+	+	+
Basic-SVR	+	+	+	+
BPNN-GD	+	+	+	+

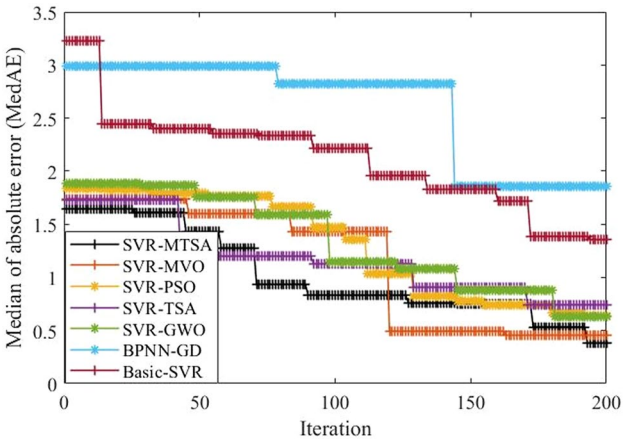

Fig. 13 The median of absolute errors for different methods over 200 iterations

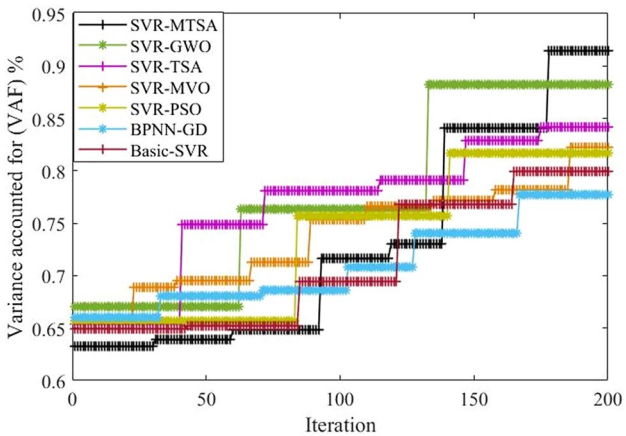

Fig. 12 The comparison of different methods in terms of VAF

values. Therefore, it can be concluded that the proposed model can predict lead recovery with reasonable accuracy for any combination of process parameters.

Sensitivity analysis using SVR-MTSA strategy

The sensitivity analysis is used to rank the effect of process parameters on the lead recovery efficiency using the proposed SVR-MTSA strategy. In this analysis, each parameter was changed between its minimum and maximum levels, while the other parameters were kept constant at their mean value. The results, shown in Fig. 15, revealed that temperature, coke content, processing time, Na_2CO_3 content, and Fe content had the most significant effect on the lead recovery efficiency, respectively.

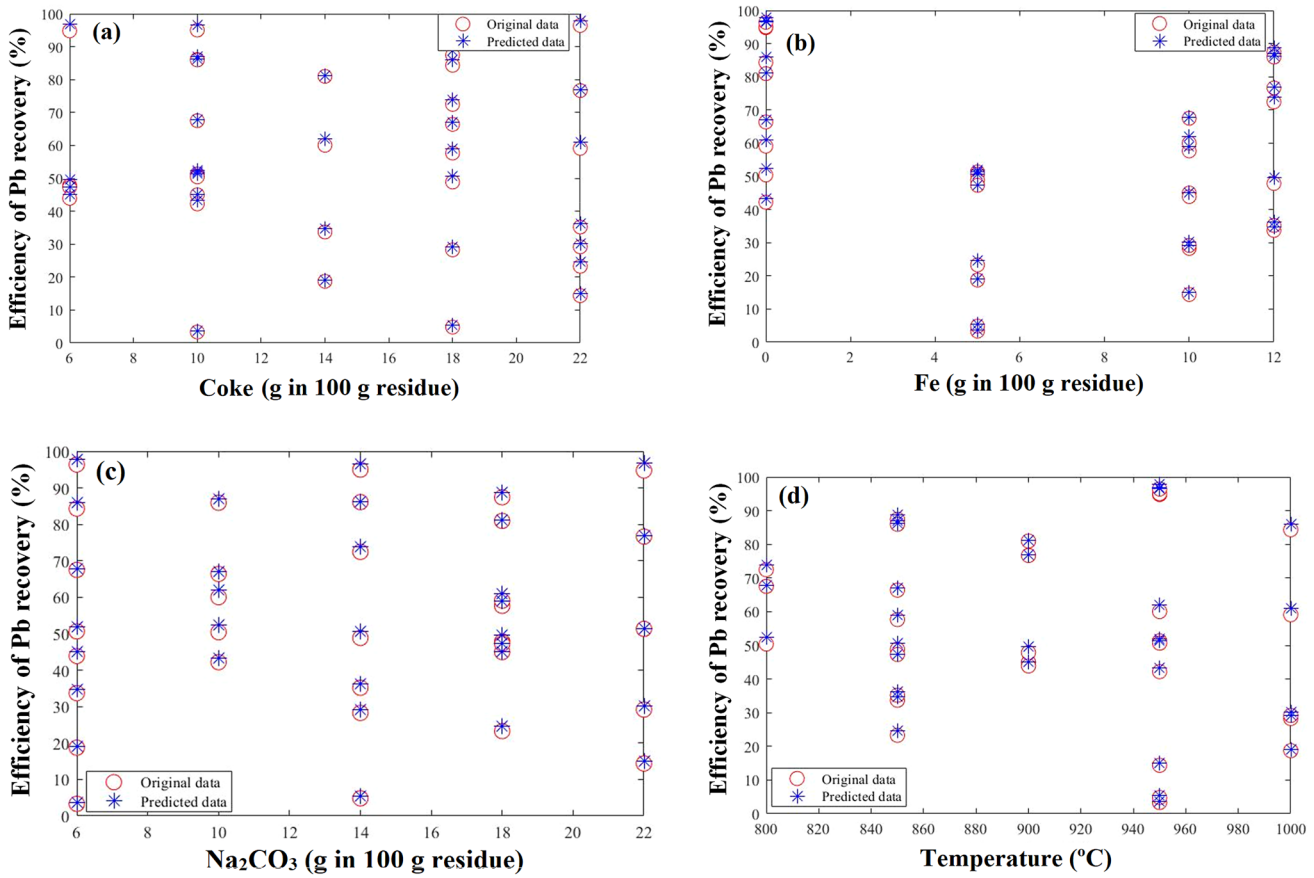

Fig. 14 Comparison of the efficiency of the Pb recovery obtained experimentally with those predicted by the SVR-MTSA for the variation in **a** processing time, **b** temperature, **c** coke, **d** Fe, and **e** Na_2CO_3 contents

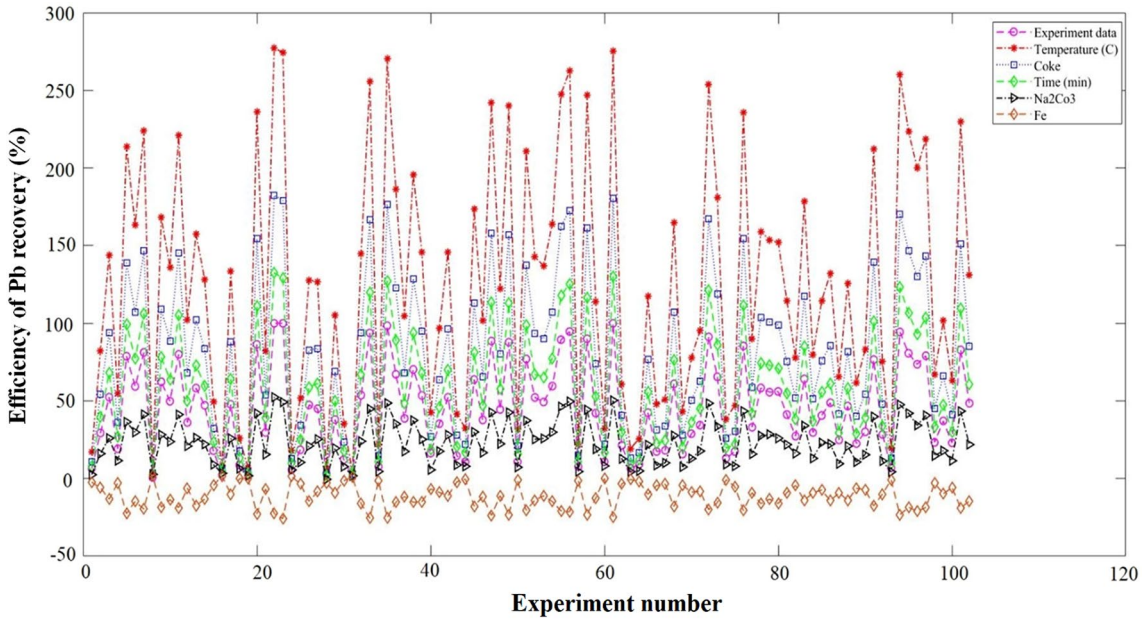

Fig. 15 The sensitivity analysis of selected features on the efficiency of Pb recovery, note: more fluctuation in each parameter means its higher impact

Comparison of the effect of experimental parameters on the lead recovery

Determining the simultaneous effect of process parameters on the efficiency of the Pb recovery process is essential. This knowledge can help the industry to choose the best combination of parameter values in any specific circumstance. In this regard, the interactions of binary parameters are evaluated using the SVR-MTSA, and the results are shown graphically in Fig. 16. It is worth noting that the values of the other parameters in each graph are kept constant at their proposed optimal values. The sensitivity analysis showed that temperature and coke content had the most significant effect on the recovery. A large portion of the figures that illustrate the binary influence of these process parameters (i.e., Fig. 16a–g)) include purple counters. While, the portion of the purple counters significantly decreased in Fig. 16c, i, and j with Fe and Na_2CO_3 at their axis. Determination of temperature and coke as the most effective process parameters implied that the amount of sulfide and oxide phases of Pb in

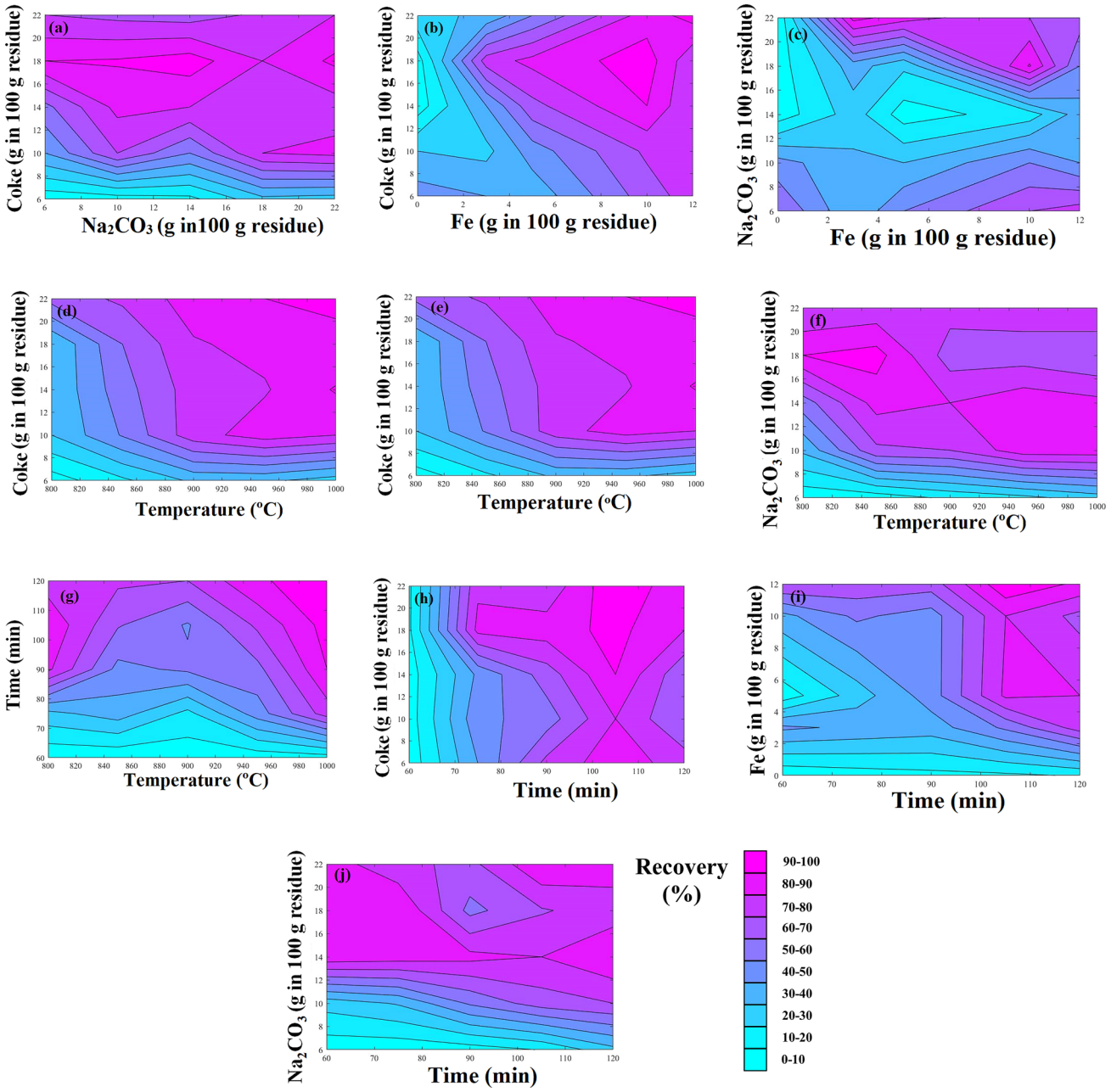

Fig. 16 Comparison of the effect of two parameters on the efficiency of Pb recovery. The value of other parameters was kept constant at their proposed optimal values ($T = 990$ °C, $t = 110$ min, Coke = 11 g/100 g and $Na_2CO_3 = 14.5$ g/100 g)

the Pb-rich waste had a determinative effect on the efficiency of the recovery.

Conclusion

In this study, a hybrid of support vector regression and a modified tunicate swarm algorithm (SVR-MTSA) strategy is developed to optimize the process parameters for recovery of Pb from the residual of the liberator cells.

1. The proposed SVR-MTSA strategy could keep a good balance between the exploration and exploitation abilities during the optimization;
2. the high ability of the proposed MTSA strategy for optimization of the SVR parameters is demonstrated;
3. the experimental results showed that the SVR-MTSR strategy could be effectively employed to predict the efficiency of the lead recovery process in any selected process parameters;
4. the sensitivity analysis of the proposed model revealed that temperature and coke content were the process parameters that had the most significant influence on the recovery of lead in the selected recovery process;
5. a recovery efficiency of higher than 99% could be achieved when the optimal process parameters for Pb recovery from the liberator cells waste were chosen using the proposed SVR-MTSA model. This recovery efficiency was higher than those obtained from the neural network model.

Declarations

Conflict of interest The authors declare that they have no known competing financial interests or personal relationships that could have appeared to influence the work reported in this paper.

References

1. Zhang X, Xie Y, Lin X, Cao H (2013) An overview on the processes and technologies for recycling cathodic active materials from spent lithium-ion batteries. J Mater Cycles Waste Manage 15:420–430. https://doi.org/10.1007/s10163-013-0140-y
2. Kreusch MA, Ponte MJJS, Ponte HA, Kaminari NMS, Marino CEB, Mymrin V (2007) Technological improvements in automotive battery recycling. Resour Conserv Recycl 52:368–380. https://doi.org/10.1016/j.resconrec.2007.05.004
3. Badawy SM, Nayl AA, El Khashab RA, El-Khateeb MA (2014) Cobalt separation from waste mobile phone batteries using selective precipitation and chelating resin. J Mater Cycles Waste Manage 16:739–746. https://doi.org/10.1007/s10163-013-0213-y
4. Chena CS, Jen SY, Hui HY (2016) Recovery of lead from smelting fly ash of waste lead-acid battery by leaching and electrowinning. Waste Manage 52:212–220. https://doi.org/10.1016/j.wasman.2016.03.056
5. Ma Y, Qiu K (2015) Recovery of lead from lead paste in spent lead acid battery by hydrometallurgical desulfurization and vacuum thermal reduction. Waste Manage 40:151–156. https://doi.org/10.1016/j.wasman.2015.03.010
6. Schlesinger ME, Sole KC, Davenport WG, King MJ (2011) Extractive Metallurgy of Copper, 5th edn. Elsevier, New York
7. Prengaman RD, Siegmund A (1999) Improved copper electrowinning operations using wrought Pb-Ca-Sn anodes, International symposium, October 10–13;1–11
8. Mirza A, Burr M, Ellis T, Evans D, Kakengela D, Webb L, Gagnon J, Leclercq F, Johnston A (2015) Corrosion of lead anodes in base metals electrowinning, Copper Cobalt Africa, incorporating the 8th Southern African Base Metals Conference Livingstone, Zambia, 6–8 July
9. Zhang J, Sato T, Iai S, Hutchinson T (2008) A pattern recognition technique for structural identification using observed vibration signals: linear case studies. Eng Struct 30:1439–1446. https://doi.org/10.1016/j.engstruct.2007.08.006
10. Mounce SR, Mounce RB, Boxall JB (2011) Novelty detection for time series data analysis in water distribution systems using support vector machines. J Hydroinf 13:672–686. https://doi.org/10.2166/hydro.2010.144
11. Boughorbel S, Tarel JP, Boujemaa N (2005) Generalized histogram intersection kernel for image recognition. IEEE Int Conf Image Process. https://doi.org/10.1109/ICIP.2005.1530353
12. De Souza DL, Granzotto MH, De Almeida GM, Oliveira-Lopes LC (2014) Fault detection and diagnosis using support vector machines—a SVC and SVR comparison. J Saf Eng 3:18–29. https://doi.org/10.5923/j.safety.20140301.03
13. Thissen U, Van Brakel R, De Weijer AP, Melssen WJ, Buydens LMC (2003) Using support vector machines for time series prediction. Chemom Intell Lab Syst 69:35–49. https://doi.org/10.1016/S0169-7439(03)00111-4
14. Hu Y, Tang Ch, Tang M, Chen Y (2015) Reductive smelting of spent lead–acid battery colloid sludge in a molten Na_2CO_3 salt. Int J Miner Metall Mater 22:798–803. https://doi.org/10.1007/s12613-015-1136-5
15. Sanchez MA, Gutiérrez PVH, Cruz RA, Sanchez RG (2016) Lead production from recycled paste of lead acid batteries with SiC-Na_2CO_3. Russ J Non-Ferr Metals 57:316–324. https://doi.org/10.3103/S1067821216040118
16. Li M, Yang J, Liang Sh, Hou H, Hu J, Liu B, Kumar R (2019) Review on clean recovery of discarded/spent lead-acid battery and trends of recycled products. J Power Sources. https://doi.org/10.1016/j.jpowsour.2019.226853
17. Li Y, Yang S, Taskinen P, He J, Liao F, Zhu R, Chen Y, Tang C, Wang Y, Jokilaakso A (2019) Novel recycling process for lead-acid battery paste without SO2 generation—reaction mechanism and industrial pilot campaign. J Clean Prod 217:162–171. https://doi.org/10.1016/j.jclepro.2019.01.197
18. Pickles CA, Toguri JM (1993) The soda ash smelting of lead-acid battery residue. Resour Conserv Recycl 9:155–177. https://doi.org/10.1016/0921-3449(93)90001-V
19. Eren Y, Küçükdemiral IB, Üstoğlu İ (2017) Chapter 2—introduction to optimization, optimization in renewable energy system. Elsevier, New York, pp 27–74. https://doi.org/10.1016/B978-0-08-101041-00002-8.tuni
20. Kaur S, Awasthi LK, Sangal AL (2020) Dhiman G (2020) Tunicate Swarm Algorithm: a new bio-inspired based metaheuristic paradigm for global optimization. Eng Appl Artif Intell. https://doi.org/10.1016/j.engappai.2020.103541
21. Shafaei A, Khayati GR (2019) A predictive model on size of silver nanoparticles prepared by green synthesis method using hybrid artificial neural network-particle swarm optimization algorithm.

Measurement S0263–224:31065–31066. https://doi.org/10.1016/j.measurement.2019.107199
22. Roh SB, Oh SK, Park EK, Choi WZ (2017) Identification of black plastics realized with the aid of Raman spectroscopy and fuzzy radial basis function neural networks classifier. J Mater Cycles Waste Manag 19:1093–1105. https://doi.org/10.1007/s10163-017-0620-6
23. Ebrahimzade H, Khayati GR, Schafe M (2018) Leaching kinetics of valuable metals from waste Li-ion batteries using neural network approach. J Mater Cycles Waste Manag 20:2117–2129. https://doi.org/10.1007/s10163-018-0766-x
24. Röpke K (2009) Design of experiments in engine development: modern development methods to meet new challenges; with 30 tables. Expert-Verlag GmbH
25. Sibanda WOL (2018) Introductory guide to design-of-experiments. Amazon Digital Services LLC—Kdp Print, US
26. Ebrahimzade H, Khayati GR, Schafe M (2020) PSO–ANN based prediction of cobalt leaching rate from waste lithium ion batteries. J Mater Cycles Waste Manage 22:228–239. https://doi.org/10.1007/s10163-019-00933-2
27. Kim JBE (2019) A new support vector machine with an optimal additive kernel. Neurocomputing 329:279–299. https://doi.org/10.1016/j.neucom.2018.10.032
28. Dhiman G, Singh KK, Soni M, Nagar A, Dehghani M, Slowik A, Kaur A, Sharma A, Houssein EH, Cengiz K (2020) MOSOA: a new multi-objective seagull optimization algorithm. Expert Syst Appl (in press). https://doi.org/10.1016/j.eswa.2020.114150
29. Ganjefar S, Tofighi M (2017) Training qubit neural network with hybrid genetic algorithm and gradient descent for indirect adaptive controller design. Eng Appl Artif Intell 65:346–360. https://doi.org/10.1016/j.engappai.2017.08.007